Chapter 10
Heterogeneous Photo-Fenton Technology

10.1 Introduction

In recent years, a lot of organic compounds have been used in industries with the rapid growth of modern science and technology, and they are inevitably released into environment, which causes great harm to human beings due to their toxicity, mutagenicity, and potential carcinogenicity [1–5]. Therefore, it is essential to remove these organic contaminants from wastewater and natural water.

Advanced oxidation processes (AOPs) need less energy than direct oxidation to degrade organic compounds [6–10]. Fenton technology is one of the most widely used methods as AOPs for the treatment of organic pollutants in water [11, 12]. Fenton oxidation process, a catalytic reaction of H_2O_2 with iron ions, mainly produces $\bullet OH$ radicals to oxidize organic compounds [13, 14], as shown in Eq. (10.1), which is considered as the core reaction in the process:

$$H_2O_2 + Fe^{2+} \rightarrow Fe^{3+} + OH^- + \bullet OH \tag{10.1}$$

The generated Fe^{3+} can be reduced by other H_2O_2 to reproduce Fe^{2+} and more radicals $HO_2\bullet$), which is called Fenton-like reaction and may account for the reason that a small amount of iron added can continue catalyzing H_2O_2 to produce $\bullet OH$ radicals, as shown in Eq. (10.2).

$$Fe^{3+} + H_2O_2 \rightarrow Fe^{2+} + HO_2\bullet + H^+ \tag{10.2}$$

There are other several reactions in Fenton oxidation process as well, as shown in Eqs. (10.3), (10.4), and (10.5):

$$Fe^{2+} + \bullet OH \rightarrow Fe^{3+} + OH^- \tag{10.3}$$

J. Zhang et al., *Photocatalysis*, Lecture Notes in Chemistry 100,
https://doi.org/10.1007/978-981-13-2113-9_10

$$Fe^{2+} + \bullet O_2H \rightarrow Fe^{3+} + HO_2^- \quad (10.4)$$

$$Fe^{3+} + \bullet O_2H \rightarrow Fe^{2+} + O_2 + H^+ \quad (10.5)$$

Therefore, hydroxyl radicals are continuously produced and are able to degrade organic compounds uninterruptedly.

However, traditional Fenton reaction has some shortcomings that are focused on (1) low efficiency in utilizing H_2O_2, (2) narrow pH range (almost Fenton reaction is conducted at pH below 3.0), (3) great loss of iron ions and formation of solid sludge ($Fe(OH)_3$ is mainly included) so that the degradation rate subsequently decreases, and (4) difficulty in recycling catalysts [15–19].

Graphene is a two-dimensional lamellar structure with one-atom-thick, which is formed as hexagon rings by sp^2-hybridized carbon atoms. The graphene was first produced by a technique called micromechanical cleavage in 2004 [20] which subsequently raised the research climax. Subsequently, several other methods based on redox process are invented, including SiC epitaxial method and chemical vapor deposition method, which makes easier to prepare graphene. Due to its honeycomb network structure, graphene has a high surface area (~2630 $m^2\ g^{-1}$), high current density (10^8 A cm^{-2}), superior mechanical properties, high thermal conductivity (~2000–5000 W m K^{-1}) [21], excellent mobility of charge carriers (~100,000 $cm^2\ V^{-1}\ s^{-1}$) [22], optical transmittance [23], super hydrophobicity at nanometer scale, etc. These excellent properties make graphene as a unique material in wide applications including batteries [24–26], solar cells [27–29], sensors [30–32], catalysts, water treatment [33–41], and so on.

Recently, graphene has been strongly focused on its application in Fenton reaction to overcome the shortcomings of traditional Fenton technique. 2D π-π conjugation of graphene can reduce the recombination rate of electrons and holes. Graphene is a prominent electron acceptor to attract the excited photoelectrons from semiconductors, which are eventually segregated with the holes. The incorporation of semiconductor nanoparticles into graphene surface limits the restacking and agglomeration of graphene, which enlarges the surface area of the composites. Meanwhile, the functional groups and defect sites of graphene as building blocks provide the nucleation and growth sites for semiconductor nanoparticles, which lead to less aggregation of semiconductor nanoparticles. Therefore, the catalytic activity of the catalyst is also enhanced due to synergistic effects between graphene and semiconductor in Fenton reaction. What is more, the combination of two materials makes the nanoparticles tightly anchored on graphene which can effectively prevent the leaching of the catalyst and make recovery easier [42–44]. Figure 10.1 illustrates the mechanism of electron transfer of graphene/metal oxide composite.

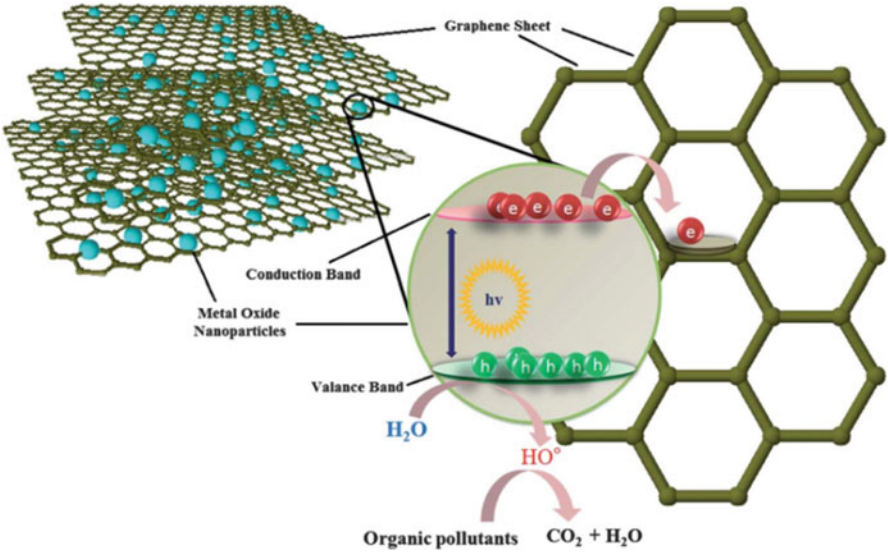

Fig. 10.1 Electron transfer from conduction band of metal oxide to graphene through percolation mechanism

10.2 Graphene/Iron (Hydr)oxide Composites Applied in Fenton Reaction

To date, a series of studies has been reported on the application of graphene/iron (hydr)oxide composites as photocatalysts to degrade organic pollutants in wastewater, especially dye pollution, which is attributed to their excellent conductivity, adsorptivity, stability, reusability, etc. Graphene has been used as an ideal support material to combine with various iron (hydr)oxides such as Fe_2O_3, Fe_3O_4, FeOOH, $ZnFe_2O_4$, and so on [45–48]. The synergistic effects of restricting electron–hole recombination and preventing the leaching of iron oxides strongly enhance the photocatalytic activity of the composite. Besides, the large plane structure of graphene makes aromatic pollution easier to be adsorbed and accelerates the process of catalysis. Thus, graphene/Fe_2O_3, graphene/Fe_3O_4, and other graphene/iron (hydr) oxides have been discussed and their photocatalytic activity has been evaluated in the following parts and tabulated in Table 10.1.

10.2.1 Graphene/Fe_2O_3 Composite as Photocatalyst in Fenton Reaction

α-Fe_2O_3 is the most widely used crystalline structure of iron oxide as it is abundant, inexpensive, and environmentally benign. α-Fe_2O_3 is an n-type semiconductor and

Table 10.1 The photocatalytic activity of various graphene/iron (hydr)oxide composites

Photocatalysts	Light source	Photocatalytic application	Photocatalytic activity enhancement	Reference
Fe_2O_3/NG	Visible light (λ > 420 nm) xenon lamp	Degradation of MB and glyphosate	1.5-fold and 2.3-fold of α-Fe_2O_3	[50]
Fe_2O_3/GO	Visible light (λ > 420 nm), 300 W Dy lamp	Degradation of Rhodamine B and 4-nitrophenol	–	[51]
α-Fe_2O_3/G	350 W xenon lamp	Degradation of RhB	2.3-fold of α-Fe_2O_3	[52]
α-Fe_2O_3/GO	UV light nm), 100 W high-pressure mercury lamp	Degradation of MB	2.9-fold of TiO_2 and 2.4-fold of α-Fe_2O_3	[53]
Fe_2O_3/GAs	Visible light (AM 1.5G), 300 W xenon lamp	Degradation of MO	–	[54]
Fe_3O_4/GO	–	Degradation of isatin	–	[61]
Fe_3O_4/RGO	Visible light (AM 1.5G), 300 W xenon lamp	Degradation of MO	More high and stable to Fe_3O_4	[62]
Fe_3O_4/RGO	Visible light (AM 1.5G), 300 W xenon lamp	Degradation of MB	–	[63]
Fe_3O_4/GO	Visible light (AM 1.5G), 500 W xenon lamp	Degradation of phenol	–	[64]
Fe_3O_4/AG	Sunlight (10.00 am ~ 2.00 pm)	Degradation of phenol, 2-NP, and 2-CP	Remarkable to the other reported nanomaterials	[65]
Fe_3O_4/HG	500 W high-voltage mercury lamp	Degradation of MO		[66]
Fe^0–Fe_3O_4–RGO	–	Degradation of MB	–	[67]
Fe_3O_4/GO	–	Degradation of AO7	–	[68]
$ZnFe_2O_4$/G	Visible light (λ > 420 nm), 300 W xenon lamp	Degradation of MB	20-fold of spinel-based photocatalysts, 4-fold of TiO_2-based photocatalysts, and 4-fold of other photocatalysts	[72]

(continued)

Table 10.1 (continued)

Photocatalysts	Light source	Photocatalytic application	Photocatalytic activity enhancement	Reference
$ZnFe_2O_4$/G	Visible light ($\lambda > 420$ nm), 500 W xenon lamp	Degradation of MB	–	[73]
$ZnFe_2O_4$/G	Visible light ($\lambda > 420$ nm), 500 W xenon lamp	Degradation of RhB, MO, and MB	–	[74]
α-FeOOH/RGO	Solar light	Degradation of phenol	–	[75]
α-FeOOH/GCA	UV light (365 nm), 125 W high-pressure mercury lamp	Degradation of MB, RdB, OII, phenol, and BPA	–	[76]

has a low bandgap of 2.2 eV so that it can absorb visible light within 560 nm, indicating it can utilize most of the visible light to oxidize organic contaminants. However, the shortcoming of α-Fe_2O_3 lies in the high electron–hole recombination rate and slow conversion of Fe (II) and Fe (III), so the catalytic activity of α-Fe_2O_3 is much poor compared to that of γ-Fe_2O_3, Fe_3O_4, and some other iron catalyst [49]. Several methods including fabricating composite with carbon material and forming yolk–shell structure with CdS realized the effective suppression of photo-generated electron and hole of α-Fe_2O_3 and make it more active in Fenton reaction.

Graphene as a single-layer carbon material has been frequently explored to prepare composites with α-Fe_2O_3 as α-Fe_2O_3/graphene composites. The large contact interface and strong interaction between graphene and α-Fe_2O_3 promote the electron transfer from α-Fe_2O_3 to graphene, which results in an enhanced photocatalytic activity. Liu et al. [50] have prepared the composite of α-Fe_2O_3 anchored on the graphene oxide (GO) nanosheet (α-Fe_2O_3/GO) (Fig. 10.2) and found that the photocatalytic activity of the composite has been enhanced, which led to approximately 2.9-fold that of classical Degussa P25 TiO_2 and 2.4-fold that of α-Fe_2O_3 for the degradation of methylene blue in Photo-Fenton reaction. Guo et al. [51] have developed a method to synthesize Fe_2O_3/GO composite at low temperature (60 °C) and found that the degradation rate of Rhodamine B and 4-nitrophenol was efficiently improved and the catalyst was potential for its good stability, little iron leaching, simple separation, stable catalytic activity, and wide pH range.

What is further reported is graphene content of the composite, which intensively influences its photocatalytic activity and other performance. Generally speaking, there is an optimal value for the composite quantity of graphene. The photocatalytic activity could be improved using graphene within a certain quantity, but it will decrease when graphene content is beyond the threshold value through enhancing absorption and scattering of photons by excess carbon content present in the composite. Han et al. [52] have explored the photocatalytic activities of the

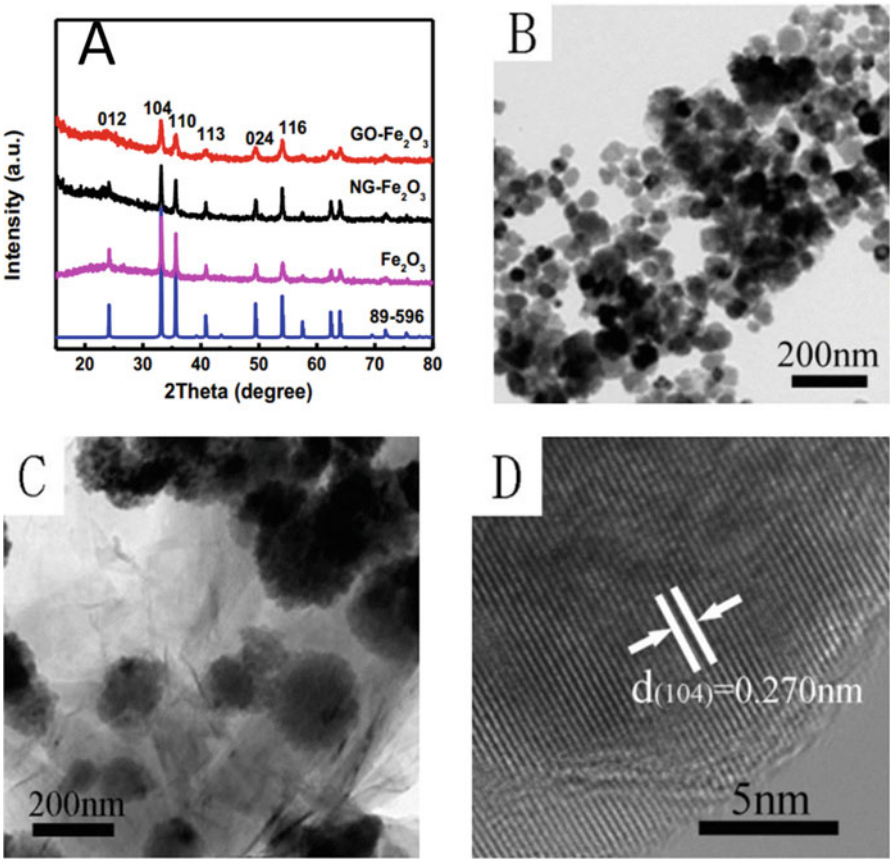

Fig. 10.2 XRD patterns (**a**), TEM image of GO-Fe_2O_3 (**b**), NG-Fe_2O_3 (**c**) and HRTEM image of NG-Fe_2O_3 (**d**). Reprinted with permission from ref. [50]. Copyright 2017, Elsevier

α-Fe_2O_3/GO composites with a serious gradient ratio of GO to α-Fe_2O_3 (0.1%, 1.0%, 2.0%, 5.0%, and 8.0%, respectively), comparing with the pure α-Fe_2O_3 nanoplates. As Fig. 10.3a shows, the absorption peak at 550 nm decreased in intensity as the time prolonged. And compared to pure α-Fe_2O_3, the value of c/c_0 decreased faster within a certain period of time when the ratio of GO increased and the composite with 5.0 wt.% of GO had the best catalytic performance shown in Fig. 10.3b and 3c, respectively. As a result, the degradation rate constant of the composite with the optimal ratio of 5 wt% graphene was almost four times faster than the pure α-Fe_2O_3 nanoplates and 98% of Rhodamine (RhB) was decomposed with 20 min of irradiation (Fig. 10.3d).

Moreover, the structure and the morphology of the graphene also affect the photocatalytic activity of the composites. A composite of α-Fe_2O_3 and graphene with N-doping has exhibited higher photocatalytic efficiency. Liu et al. [53] have reported a pyrrolic N-doped graphene oxide/Fe_2O_3 mesocrystal (NG-Fe_2O_3)

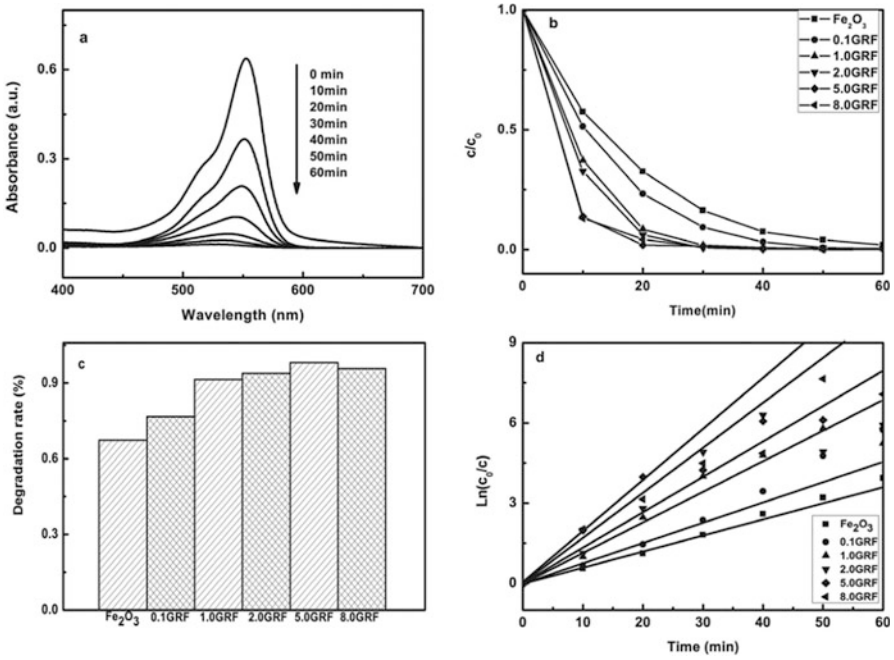

Fig. 10.3 (**a**) Time-dependent UV-vis absorption spectra in the presence of α-Fe_2O_3 under Xe light irradiation. (**b**) Photodegradation of RhB by α-Fe_2O_3 and α-Fe_2O_3/graphene composites under Xe light irradiation 60 min. (**c**) Comparison of photocatalytical performance of α-Fe_2O_3 and α-Fe_2O_3/graphene composites in 20 min. (**d**) Kinetic curves of the degradation of RhB by α-Fe_2O_3 and α-Fe_2O_3/graphene composites. Reprinted with permission from ref. [52]. Copyright 2014, Wiley

nanocomposite which showed 1.5 times higher on degrading methyl blue and 2.3 times higher on converting glyphosate. There are two reasons to explain: (1) the content of the oxygen-containing groups on GO had been adjusted and the morphology of NG-Fe_2O_3 has been changed a larger BET surface area compared to that of bare Fe_2O_3 and (2) the intimating contact between Fe_2O_3 and NG accelerated the electron transfer from Fe_2O_3 to NG so that the holes in Fe_2O_3 were increased to accept electrons from H_2O_2 to generate hydroxyl radicals in Photo-Fenton reaction. Thus, the photocatalytic efficiency was improved as observed.

Recently, Fe_2O_3/3D graphene aerogels (GAs) have been widely studied, but most of researches have been done on lithium ion batteries due to the difficulty in dispersing Fe_2O_3 particles on 3D-graphene, which limits its application in Photo-Fenton reaction. Qiu et al. [54] have solved the problem of dispersion of Fe_2O_3 particles on GAs by a modified Stöber-like method. Such 3D network structure inhibited Fe(II) loss and stabilized the conversion of Fe(III)/Fe(II) in Photo-Fenton reaction. Besides, the composite was full of elasticity and easy to be recycled shown in Fig. 10.4, and the loss of Fe(II) of Fe_2O_3/GR ordinary composite remained high in acidic solution, which led to the deactivation of the catalyst and degradation rate of organic contaminants. Thus, compared to pure Fe_2O_3 and Fe_2O_3/GR with the similar

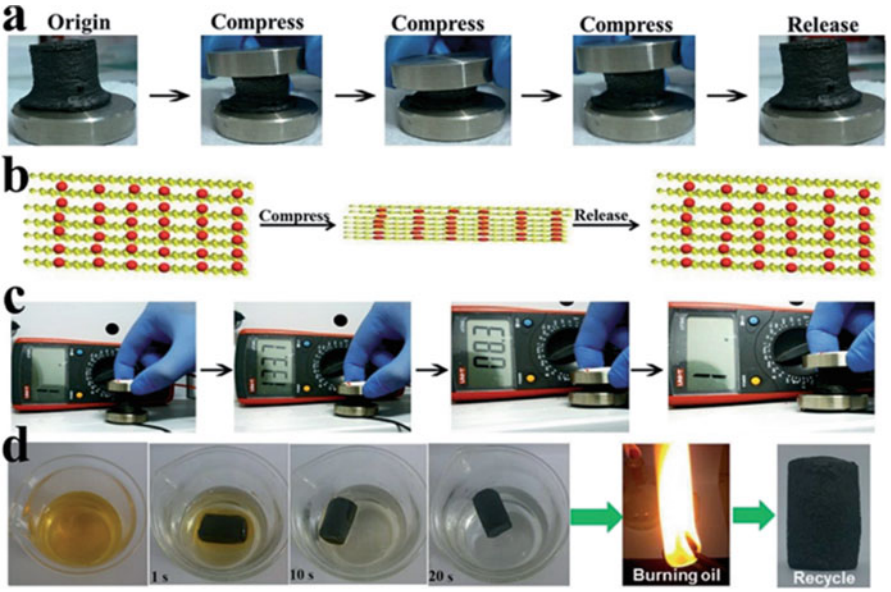

Fig. 10.4 (**a**) Compression test of Fe_2O_3/GAs. (**b**) Schematic illustration of the structure of Fe_2O_3/GAs during the compression test. (**c**) The changing impedance of Fe_2O_3/GAs during the compression process. (**d**) Sequential images of Fe_2O_3/GAs absorbing pump oil (dyed with Sudan III) on a water surface and the recycling of Fe_2O_3/GAs through burning off the oil. Reprinted with permission from ref. [54]. Copyright 2015, Royal Society of Chemistry

particle size and concentration, Fe_2O_3/GAs exhibited higher Photo-Fenton reaction activity after the several cycles.

10.2.2 Graphene/Fe_3O_4 Composite as Photocatalyst in Fenton Reaction

Fe_3O_4, a magnetic material with a structure of inverse spinal, is regarded as the most promising catalyst in Fenton-like reaction due to its decent magnetic, electric, and catalytic properties, biocompatibility, and low toxicity [55, 56] The octahedral structure contains both Fe^{2+} and Fe^{3+} and the electrons can move fast between them, allowing the Fe species to be selectively reduced or oxidized and keeping the structure invariant at the same time. In addition, the narrow bandgap (0.1 eV) of Fe_3O_4 is of great importance to electron carrier and magnetic properties of Fe_3O_4 cause it to be easily dispersed by an external magnetic field, both of which can enhance photocatalytic activity. However, the nanoscaled Fe_3O_4 particles are prone to aggregate to become larger particles that will lose its initial huge surface area and dispersibility in the aqueous solution and finally diminish the photocatalytic activity toward organic pollutants. Meanwhile, the slow conversion rate of Fe(II) and Fe(III)

limits the reaction rate of Fenton process which is the control step and key procedure to enhance the catalytic capacity of Fe_3O_4 NPs [57–60].

In order to overcome these drawbacks, methods like immobilizing Fe_3O_4 nanoparticles onto support materials or encapsulating them within thin protective layer to prevent their aggregation and electron acceptors are utilized to accelerate the electron transfer. Naturally, carbon materials, especially graphene, attract the focus of chemical researchers again, which not only can be supporters to anchor nanoparticles but also acceptors to receive electrons. Several researches have reported that the in situ growth of Fe_3O_4 NPs onto graphene can not only effectively inhibit the aggregation of magnetite but also enable them to contact with each other intimately, and such structure favored the transmission of photoactive electrons from Fe_3O_4 NPs to graphene. The magnetite nanoparticles are dispersed on the GO (or rGO) sheets and immobilized by ferric or ferrous ions bonded with oxygen-containing functional group as crystal nucleuses, which will be the active sites for catalysis. Herein, the surface area of magnetite is enlarged and the surface energy-derived agglomeration of nanosized particles is prevented by graphene sheets. In return, Fe_3O_4 NPs with certain size can avoid accumulation of adjacent graphene sheets. Zhou et al. [61] have successfully synthesized GO-Fe_3O_4 composite through in situ depositing cubic-phase Fe_3O_4 on the surface of GO and proved the existence of the C–O–Fe coordination bond by FTIR. The composite showed excellent performance on photocatalytic degrading organic contaminant isatin. In another study, Qiu et al. [62] reported a simple Stöber-like method without additional reductants and organic surfactants on the synthesis of rGO–Fe_3O_4 nanocomposite, which was environmental friendly and suitable for mass production. The Fe_3O_4 NPs were ultra-dispersed on the graphene sheets during the in situ growth process and the particle sizes were well controlled at an extremely small value (3–8 nm), which was clearly seen in Fig. 10.5. The results of Photo-Fenton experiments to degrade methyl orange, methylene blue, and Rhodamine B were satisfactory due to the high surface area and fast electron transfer.

The graphene content in the magnetite-based composites also plays one of the decisive factors for the performance of photocatalyst. There is no doubt that the graphene content of the composite has an optimal value for the sake of the highest photocatalytic activity similar to combination with Fe_2O_3 above. Zubir et al. [63] have found that the beneficial intercalation of GO within Fe_3O_4 nanoparticles was 10 wt% after a series of experiments using composites with different weight ratio of GO to degrade organic compounds, which showed 20% higher degradation rate of Acid Orange 7 than that of bare Fe_3O_4 nanoparticles, as well (Fig. 10.6a). This can be explained that at high GO loading, stacking of the graphene sheets may happen through the π-π interactions which correspond to the van der Waals and hydrophobic fields around the carbon basal plane of GO sheets. Therefore, the aggregation of Fe_3O_4 NPs on the exterior surface of GO stacking might hamper the effective diffusion and contact between the reactants toward the active sites and decrease the ample formation of hydroxyl radicals to decompose AO7 during the reaction. The pH range was extended to nearly neutral condition and the cyclicity of the composite was perfect as shown in Fig. 10.6b and 6c. Likewise, Yu et al. [64]

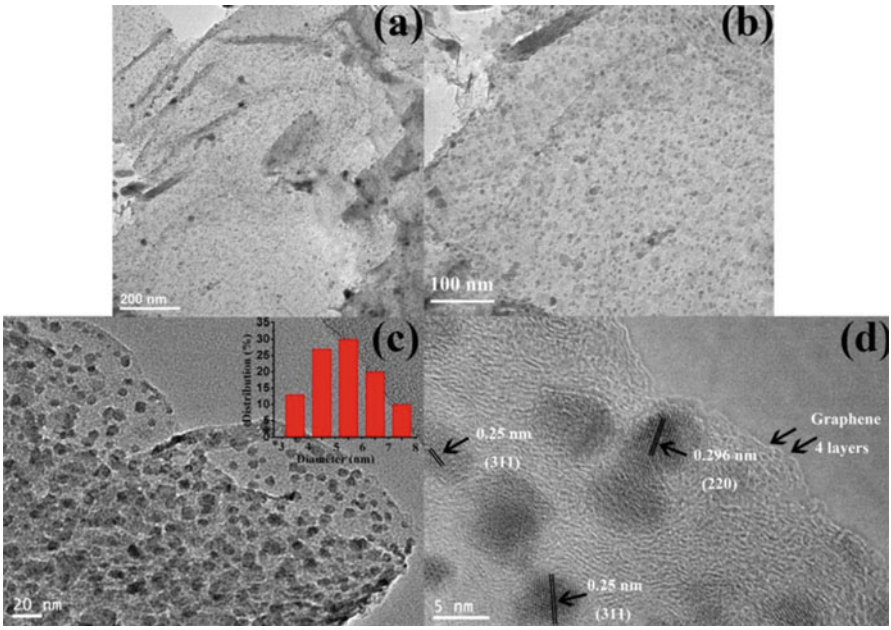

Fig. 10.5 TEM images (**a**, **b**) and HRTEM images (**c**, **d**) of Fe_3O_4/RGO composites. Inset of (**c**) is the corresponding particle size distribution of the loaded Fe_3O_4 nanoparticles derived from 100 of Fe_3O_4 nanoparticles in (**c**). Reprinted with permission from ref. [62]. Copyright 2016, Elsevier

comparatively studied the influence of the weight ratio of GO in Fe_3O_4-based composite ranging from 0 to 15 wt% on the photocatalytic activity. The result showed that the degradation rate reached the highest value when the GO content is 5 wt% in Fe_3O_4/GO composite regardless of increasing or decreasing GO content because the active sites may be covered and the contact with H_2O_2 may be hindered by superfluous GO.

In several reports, the composite of Fe_3O_4 nanoparticles combining with modified graphene shows the more efficient photocatalysis than ordinary Fe_3O_4/GO catalyst. The introduction of other functional groups or elements into graphene may facilitate the higher catalytic activity and conductivity of graphene and subsequently reinforce the capability of prohibiting the electron–hole recombination rate and adsorbing organic contaminants onto the sheets with compositing with Fe_3O_4 nanoparticles. Boruah et al. [65] synthesized AG/Fe_3O_4 composite that graphene was decorated with ammonia. The new catalyst exhibited efficient photocatalytic activity degradation of phenol, 2-nitrophenol (2-NP), and 2-chlorophenol (2-CP) and further high removal of three organic compounds under sunlight irradiation, which was attributed to the synergistic effect between AG and Fe_3O_4 NPs by preventing the recombination of electron–hole pair to enhance the catalytic performance. The synthetic route and the mechanism of degradation were presented in Fig. 10.7. Graphene could not form a good composite with Fe_3O_4 due to its hydrophobicity, so Wang et al. [66] prepared a type of hydrophilic graphene (HG) by GO reacting with

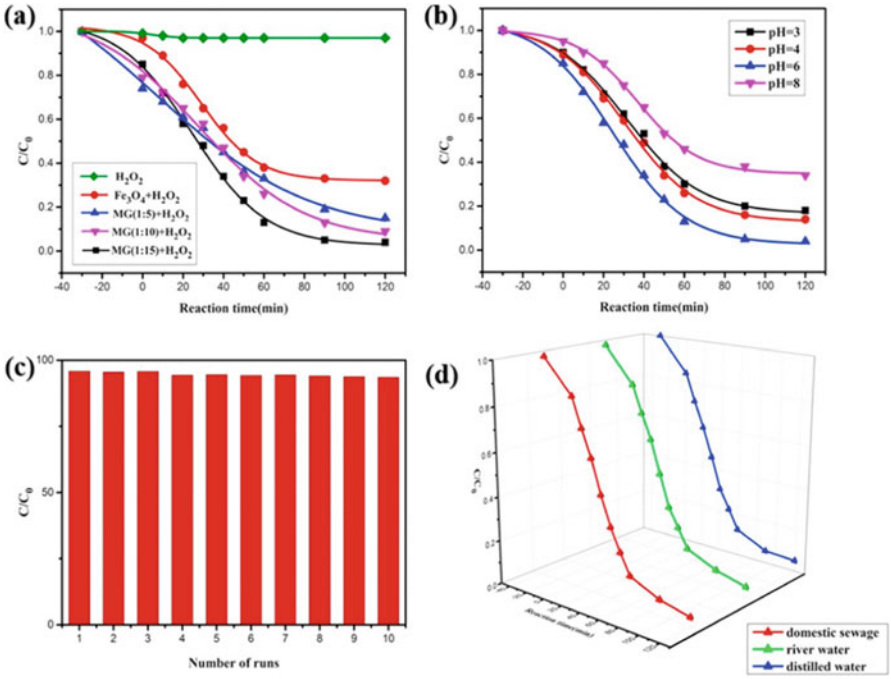

Fig. 10.6 (a) Effect of RGO content in RGO/Fe_3O_4 catalyst ($[MB]_0$ = 20 mg L^{-1}; $[H_2O_2]_0$ = 10 mmol L^{-1}; [catalyst] = 0.25 g L^{-1}; pH = 6; room temperature). (b) Degradation efficiency in different pH($[MB]_0$ = 20 mg L^{-1}; $[H_2O_2]_0$ = 10 mmol L^{-1}; [catalyst] = 0.25 g L^{-1}; room temperature). (c) Degradation rate for each run with RGO/Fe_3O_4 catalyst ($[MB]_0$ = 20 mg L^{-1}; $[H_2O_2]_0$ = 10 mmol L^{-1}; [catalyst] = 0.25 g L^{-1}; pH = 6; room temperature). (d) Degradation rate in actual water sample ($[MB]_0$ = 20 mg L^{-1}; $[H_2O_2]_0$ = 10 mmol L^{-1}; [catalyst] = 0.25 g L^{-1}; pH = 6; room temperature). Reprinted with permission from ref. [63]. Copyright 2017, Elsevier

phenylhydrazine-4-sulfonic acid to synthesize HG/Fe_3O_4 composite. The result showed that Fe_3O_4 nanoparticles were uniformly and tightly clinched onto the HG sheets, and the composites demonstrated paramagnetic characteristic, better stability in water, and higher Photo-Fenton activity.

After years of research, a variety of preparation methods of Fe_3O_4 and graphene-based catalyst have been invented in order to improve the photocatalytic efficiency in Fenton reaction, cost saving, and environmental friendly. Santhosh et al. [67] prepared G–Fe_3O_4 composite through a one-step solvothermal route, which was more convenient and less contaminative compared to two (or more)-step routes. Fe_3O_4 was proved to anchor firmly and well dispersedly on the graphene sheets in the resulting G–Fe_3O_4 composite which showed excellent performance on adsorbing heavy metal like lead ion and degrading methylene blue due to the inhibition of electron–hole recombination and more active sites for degradation. Jiang et al. [68] studied the fabrication of rGO–Fe_3O_4 nanocomposite through a creative procedure that utilized a brown alga (*Sargassum thunbergii*) as the solely reducing agent,

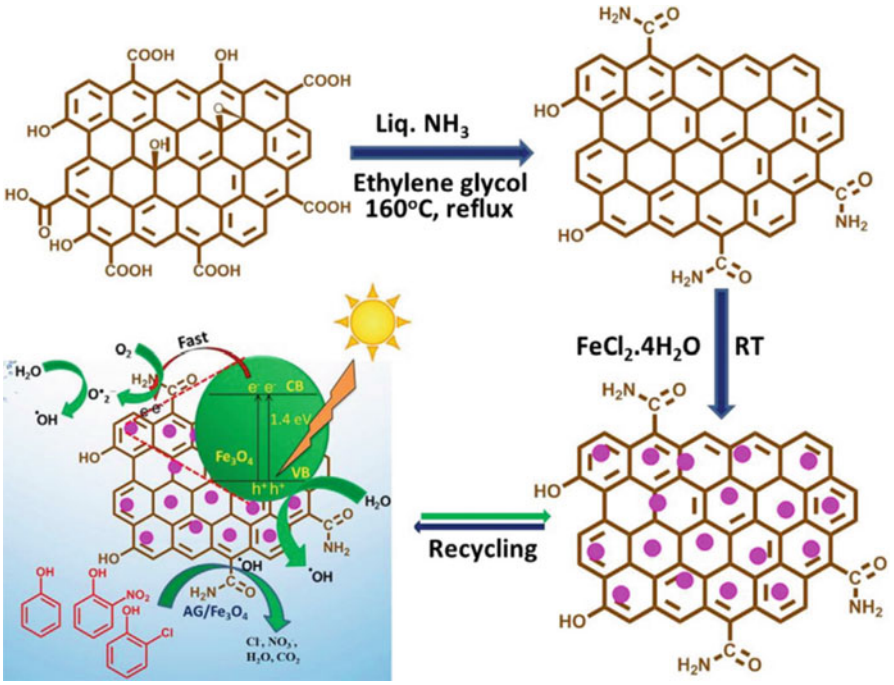

Fig. 10.7 Schematic representation for the synthesis of AG/Fe_3O_4 nanocomposite toward photocatalytic degradation of phenol, 2-NP, and 2-CP under sunlight irradiation. Reprinted with permission from ref. [65]. Copyright 2017, Elsevier

which replaced the toxic acids and amines to avoid polluting the environment. Besides, *Sargassum thunbergii* is so abundant across the coast of China that the photocatalyst can be mass prepared with low cost. This method can be regarded as the exploration on green synthetic technology and has potential of further research. The synthesized material displayed excellent catalytic performance, showing 96% degradation rate under mild conditions. Except the methods mentioned above, there are several other ideas such as hydrothermal method and co-participation method, etc., which facilitate the wide application of rGO–Fe_3O_4 as photocatalyst.

10.2.3 Graphene/Other Iron (Hydr)oxide Composite as Photocatalyst in Fenton Reaction

In addition to the above composites, other iron (hydr)oxides have also been incorporated with graphene to prepare highly effective photocatalysts for Photo-Fenton reaction. For instance, $ZnFe_2O_4$ [69], $MnFe_2O_4$ [70], and $CoFe_2O_4$ [71] with spinel structure have attracted much attention for their visible light-driven photoactivity.

Besides, α-FeOOH and β-FeOOH [48] are also explored to apply as catalyst for water purification.

$ZnFe_2O_4$ has a narrow bandgap of 1.9 eV so that it can absorb visible light up to 653 nm, which tremendously enhances the utilization of sunlight. $ZnFe_2O_4$ has great potential to be used as a high-performance photocatalyst to deal with water organic pollution owing to its high catalytic capability, low cost, and simple magnetic separation. Besides, graphene is utilized as support material and electron acceptor for $ZnFe_2O_4$. The nanosized $ZnFe_2O_4$ particles that grew on graphene have high surface area and low electron–hole recombination due to its suitable short diameter. The photo-generated electrons are rapidly transferred to graphene so that the holes are preserved to react with H_2O_2 and H_2O to generate hydroxyl radicals for decomposition of dye pollution. Furthermore, both the aggregation of $ZnFe_2O_4$ and the stack of graphene sheets were prevented. Yang et al. [72] reported a novel strategy to synthesize G-$ZnFe_2O_4$ composite through interface engineering. They used graphene as barrier to control the growth of $ZnFe_2O_4$, channels to transport photo-generated electrons, and vessels to inhibit the recombination of electrons and holes. The results showed that the G-$ZnFe_2O_4$ catalyst had an ultrafast degradation rate of methyl blue, which was 20 times higher than the previous reported spinel-based photocatalysts, 4 times higher than that of the TiO_2-based photocatalysts, and 4 times higher than those of the other photocatalysts. Fu et al. [73] prepared a magnetically separable $ZnFe_2O_4$–graphene nanocomposite photocatalyst through a facile one-step hydrothermal method (Fig. 10.8). The degradation rate of methyl blue was 88% in just 5 min and reached 99% after 90 min visible light irradiation but also concluded that compared with pure $ZnFe_2O_4$ catalyst, the as-prepared photocatalyst had a dual function of photocatalytic decomposing MB and photo-generating hydroxyl radicals. Lu and cooperators [74] obtained a $ZnFe_2O_4$–G composite with $ZnFe_2O_4$ nanocrystals simultaneously anchored on rGO by a facile one-pot solvothermal method. Similarly, the $ZnFe_2O_4$–G composite presented powerful photocatalytic activity for degradation of Rhodamine B, methyl orange, and methylene blue by Photo-Fenton reaction and could be easily recycled by an external magnetic field due to its excellent magnetism, for which the photocatalyst had the potential to be applied in water treatment.

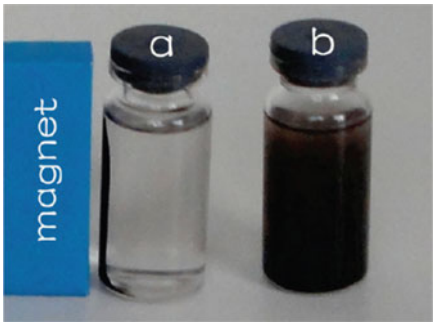

Fig. 10.8 Images of $ZnFe_2O_4$–G(0.2) suspension with (a) and without (b) a magnetic field. Reprinted with permission from ref. [73]. Copyright 2011, American Chemical Society

In recent studies, α-FeOOH has been found to degrade some recalcitrant organic compounds at neutral to alkaline pH values under UV irradiation. It first absorbs UV light to produce electrons and holes and subsequently reacts with H_2O and H_2O_2 to produce ●OH radicals. The hydroxyl radicals can also be generated by breaking up the FeO–OH bond through UV irradiation. Importantly, the incorporation of graphene and α-FeOOH enables the composite to have visible light response and absorption characteristics, and the photo-generated electrons are also transported to graphene sheets to reduce their recombination and enhance the photocatalytic activity. Wang et al. [75] prepared GO/α-FeOOH composite by reducing Fe (II) onto GO via in situ self-assembly process. They demonstrated that the as-prepared catalyst had a high activity on oxidizing phenol under visible light irradiation in a wide pH range. Liu et al. [76] synthesized α-FeOOH@GCA by incorporating GO-CNTs and α-FeOOH nanoparticles using a facile in situ hydrolysis route. Compared with pristine α-FeOOH, the composite was proved to show more effective in H_2O_2 activity and more excellent performance on degrading OII.

10.3 Conclusions and Outlook

In summary, various iron-based oxides/graphene composites have been explored to obtain more effective, environmental friendly, cheaper, and more toxic catalyst in order to solve the problem of increasingly dye pollution in water. The synergistic effect of graphene and iron (hydr)oxides semiconductors enhances the photocatalytic activity of iron (hydr)oxides to degrade a large number of water dye pollutants such as methyl blue, phenol, and so forth. The combination of the size-dependent property of nanomaterials and the excellent properties of graphene endow the composites exhibiting much more functionalities, such as large surface area, wide pH reaction range, wide sunlight response and absorption, high adsorption capacity, high speed of electron transportation, low recombination of electrons and holes, and so on. The iron (hydr)oxides have various bandgap ranging from 0.1 eV (Fe_3O_4) to 2.8 eV (FeOOH) and the potential of the minimum conductive band is more negative than the water reduction potential (H^+/H_2) or the potential of the maximum valence band is more positive than the water oxidation potential (H_2O/O_2). A variety of synthetic methods have been studied to produce iron (hydr)oxides-based composites. However, there are still some problems needed to be overcome for large-scale application. For instance, it is difficult to obtain high purified graphene with precisely controlling the defects and defect sites. The recombination of electrons and holes and restacking of graphene to graphite are not completely solved. It still needs to be further researched to find new methods to overcome the problems mentioned above.

The exploration of new catalysts and treatment technique of the organic pollutants in wastewater is an exciting and difficult work for scientific researchers. Considering the recycling of catalysts, magnetic materials may attract more attention due to that they not only possess the catalytic performance but also can be magnetic

separated by an external magnetic field, which makes them better for recycling and reduces the secondary pollution to the environment. Besides, graphene-based materials are promising and potential for water purification and also considered as future materials, but there are still lots of uncertainties to completely understand its properties and phenomenon. Water quality is quite important for human health. Therefore, Fe_2O_3, Fe_3O_4, and other iron oxides coupled with graphene are discussed and reviewed in this article to summarize the former research achievements in related fields and also to understand the properties and performance of these composites.

References

1. Speth DR, In't Zandt MH, Guerrero-Cruz S et al (2016) Genome-based microbial ecology of anammox granules in a full-scale wastewater treatment system. Nat Commun 7:11172
2. Gago-Ferrero P, Schymanski EL, Bletsou AA et al (2015) Extended suspect and non-target strategies to characterize emerging polar organic contaminants in raw wastewater with LC-HRMS/MS. Environ Sci Technol 49(20):12333–12341
3. Ojha DP, Joshi MK, Kim HJ (2017) Photo-Fenton degradation of organic pollutants using a zinc oxide decorated iron oxide/reduced graphene oxide nanocomposite. Ceram Int 43 (1):1290–1297
4. Hoffmann MR, Martin ST, Choi W et al (1995) Environmental applications of semiconductor photocatalysis. Chem Rev 95(1):69–96
5. Legrini O, Oliveros E, Braun AM (1993) Photochemical processes for water treatment. Chem Rev 93(2):671–698
6. Wu K, Xie Y, Zhao J et al (1999) Photo-Fenton degradation of a dye under visible light irradiation. J Mol Catal A-Chem 144(1):77–84
7. Neyens E, Baeyens J (2003) A review of classic Fenton's peroxidation as an advanced oxidation technique. J Hazard Mater 98(1):33–50
8. Tian S, Tu Y, Chen D et al (2011) Degradation of Acid Orange II at neutral pH using Fe2 (MoO4)3 as a heterogeneous Fenton-like catalyst. Chem Eng J 169(1):31–37
9. Feng J, Hu X, Yue P (2004) Discoloration and mineralization of Orange II using different heterogeneous catalysts containing Fe: a comparative study. Environ Sci Technol 38 (21):5773–5778
10. Arnold SM, Hickey WJ, Harris RF (1995) Degradation of atrazine by Fenton's reagent: condition optimization and product quantification. Environ Sci Technol 29(8):2083–2089
11. Herney-Ramirez J, Vicente MA, Madeira LM (2010) Heterogeneous photo-Fenton oxidation with pillared clay-based catalysts for wastewater treatment: a review. Appl Catal B-Environ 98 (1):10–26
12. Pouran SR, Aziz ARA, Daud WMAW (2015) Review on the main advances in photo-Fenton oxidation system for recalcitrant wastewaters. J Ind Eng Chem 21:53–69
13. Babuponnusami A, Muthukumar K (2014) A review on Fenton and improvements to the Fenton process for wastewater treatment. J Environ Chem Eng 2(1):557–572
14. Dhakshinamoorthy A, Navalon S, Alvaro M et al (2012) Metal nanoparticles as heterogeneous Fenton catalysts. ChemSusChem 5(1):46–64
15. Li D, Yuranova T, Albers P et al (2004) Accelerated photobleaching of Orange II on novel (H5FeW12O40•10H2O)/silica structured fabrics. Water Res 38(16):3541–3550
16. Sabhi S, Kiwi J (2001) Degradation of 2, 4-dichlorophenol by immobilized iron catalysts. Water Res 35(8):1994–2002
17. Hu X, Liu B, Deng Y et al (2011) Adsorption and heterogeneous Fenton degradation of 17α-methyltestosterone on nano Fe3O4/MWCNTs in aqueous solution. Appl Catal B-Environ 107(3):274–283

18. Timofeeva MN, Hasan Z, Orlov AY et al (2011) Fe-containing nickel phosphate molecular sieves as heterogeneous catalysts for phenol oxidation and hydroxylation with H2O2. Appl Catal B-Environ 107(1):197–204
19. Song Z, Wang N, Zhu L et al (2012) Efficient oxidative degradation of triclosan by using an enhanced Fenton-like process. Chem Eng J 198:379–387
20. Novoselov KS, Geim AK, Morozov SV et al (2004) Electric field effect in atomically thin carbon films. Science 306(5696):666–669
21. Nika DL, Pokatilov EP, Askerov AS et al (2009) Phonon thermal conduction in graphene: role of Umklapp and edge roughness scattering. Phys Rev B 79(15):155413
22. Mayorov AS, Gorbachev RV, Morozov SV et al (2011) Micrometer-scale ballistic transport in encapsulated graphene at room temperature. Nano Lett 11(6):2396–2399
23. Li X, Zhu Y, Cai W et al (2009) Transfer of large-area graphene films for high-performance transparent conductive electrodes. Nano Lett 9(12):4359–4363
24. Wang H, Cui LF, Yang Y et al (2010) Mn3O4-graphene hybrid as a high-capacity anode material for lithium ion batteries. J Am Chem Soc 132(40):13978–13980
25. Yoo EJ, Kim J, Hosono E et al (2008) Large reversible Li storage of graphene nanosheet families for use in rechargeable lithium ion batteries. Nano Lett 8(8):2277–2282
26. Liang M, Zhi L (2009) Graphene-based electrode materials for rechargeable lithium batteries. J Mater Chem 19(33):5871–5878
27. Wang X, Zhi L, Müllen K (2008) Transparent, conductive graphene electrodes for dye-sensitized solar cells. Nano Lett 8(1):323–327
28. Yin Z, Wu S, Zhou X et al (2010) Electrochemical deposition of ZnO nanorods on transparent reduced graphene oxide electrodes for hybrid solar cells. Small 6(2):307–312
29. Wu J, Becerril HA, Bao Z et al (2008) Organic solar cells with solution-processed graphene transparent electrodes. Appl Phys Lett 92(26):237
30. Schedin F, Geim AK, Morozov SV et al (2007) Detection of individual gas molecules adsorbed on graphene. Nat Mater 6(9):652–655
31. Shao Y, Wang J, Wu H et al (2010) Graphene based electrochemical sensors and biosensors: a review. Electroanalysis 22(10):1027–1036
32. Shan C, Yang H, Song J et al (2009) Direct electrochemistry of glucose oxidase and biosensing for glucose based on graphene. Anal Chem 81(6):2378–2382
33. An J, Zhu L, Wang N et al (2013) Photo-Fenton like degradation of tetrabromobisphenol A with graphene BiFeO3 composite as a catalyst. Chem Eng J 219:225–237
34. Zhou Q, Xing A, Li J et al (2016) Synergistic enhancement in photoelectrocatalytic degradation of bisphenol A by CeO2 and reduced graphene oxide co-modified TiO2 nanotube arrays in combination with Fenton oxidation. Electrochim Acta 209:379–388
35. Qiu B, Deng Y, Du M et al (2016) Ultradispersed cobalt ferrite nanoparticles assembled in graphene aerogel for continuous photo-Fenton reaction and enhanced lithium storage performance. Sci Rep-UK 6:29099
36. Babu SG, Vinoth R, Neppolian B et al (2015) Diffused sunlight driven highly synergistic pathway for complete mineralization of organic contaminants using reduced graphene oxide supported photocatalyst. J Hazard Mater 291:83–92
37. Wan Z, Hu J, Wang J (2016) Removal of sulfamethazine antibiotics using Ce Fe-graphene nanocomposite as catalyst by Fenton-like process. J Environ Manag 182:284–291
38. Wang Y, Yu Y, Deng C et al (2015) Synthesis of mesoporous MCM-41 supported reduced graphene oxide-Fe catalyst for heterogeneous Fenton degradation of phenol. RSC Adv 5 (126):103989–103998
39. Yun S, Lee YC, Park HS (2016) Phase-controlled iron oxide nanobox deposited on hierarchically structured graphene networks for lithium ion storage and photocatalysis. Sci Rep 6:19959
40. Zhou Y, Xiao B, Liu SQ et al (2016) Photo-Fenton degradation of ammonia via a manganese–iron double-active component catalyst of graphene–manganese ferrite under visible light. Chem Eng J 283:266–275
41. He H, He Z, Shen Q (2017) Photocatalysis of novel reduced graphene oxide-CoSe nanocomposites with efficient interface-induced effect. Compo Interf 24(1):85–97

42. Lee C, Wei X, Kysar JW et al (2008) Measurement of the elastic properties and intrinsic strength of monolayer graphene. Science 321(5887):385–388
43. Zheng Y, Wei N, Fan Z et al (2011) Mechanical properties of grafold: a demonstration of strengthened graphene. Nanotechnology 22(40):405701
44. Geim AK, MacDonald AH (2007) Graphene: exploring carbon flatland. Phys Today 60 (8):35–41
45. Liu Q, Guo Y, Chen Z et al (2016) Constructing a novel ternary Fe (III)/graphene/gC3N4 composite photocatalyst with enhanced visible-light driven photocatalytic activity via interfacial charge transfer effect. Appl Catal B-Environ 183:231–241
46. Zubir NA, Motuzas J, Yacou C et al (2016) Graphene oxide with zinc partially substituted magnetite (GO–Fe1−xZnxOy) for the UV-assisted heterogeneous Fenton-like reaction. RSC Adv 6(50):44749–44757
47. Lee YC, Chang SJ, Choi MH et al (2013) Self-assembled graphene oxide with organo-building blocks of Fe-aminoclay for heterogeneous Fenton-like reaction at near-neutral pH: a batch experiment. Appl Catal B-Environ 142:494–503
48. Xiao F, Li W, Fang L et al (2016) Synthesis of akageneite (beta-FeOOH)/reduced graphene oxide nanocomposites for oxidative decomposition of 2-chlorophenol by Fenton-like reaction. J Hazard Mater 308:11–20
49. Mishra M, Chun DM (2015) α-Fe2O3 as a photocatalytic material: a review. Appl Catal A-Gen 498:126–141
50. Liu B, Tian L, Wang R et al (2017) Pyrrolic-N-doped graphene oxide/Fe2O3 mesocrystal nanocomposite: efficient charge transfer and enhanced photo-Fenton catalytic activity. Appl Surf Sci 2017 412:207–213
51. Guo S, Zhang G, Guo Y et al (2013) Graphene oxide-Fe2O3 hybrid material as highly efficient heterogeneous catalyst for degradation of organic contaminants. Carbon 60:437–444
52. Han S, Hu L, Liang Z et al (2014) One-step hydrothermal synthesis of 2D hexagonal nanoplates of α-Fe2O3/graphene composites with enhanced photocatalytic activity. Adv Funct Mater 24 (36):5719–5727
53. Liu Y, Jin W, Zhao Y et al (2017) Enhanced catalytic degradation of methylene blue by α-Fe2O3/graphene oxide via heterogeneous photo-Fenton reactions. Appl Catal B-Environ 206:642–652
54. Qiu B, Xing M, Zhang J (2015) Stöber-like method to synthesize ultralight, porous, stretchable Fe2O3/graphene aerogels for excellent performance in photo-Fenton reaction and electrochemical capacitors. J Mater Chem A 3(24):12820–12827
55. Santhosh C, Kollu P, Doshi S et al (2014) Adsorption, photodegradation and antibacterial study of graphene-Fe3O4 nanocomposite for multipurpose water purification application. RSC Adv 4 (54):28300–28308
56. Shen J, Li Y, Zhu Y et al (2016) Aerosol synthesis of Graphene-Fe3O4 hollow hybrid microspheres for heterogeneous Fenton and electro-Fenton reaction. J Environ Chem Eng 4 (2):2469–2476
57. Hua Y, Wang S, Xiao J et al (2017) Preparation and characterization of Fe3O4/gallic acid/graphene oxide magnetic nanocomposites as highly efficient Fenton catalysts. RSC Adv 7 (46):28979–28986
58. Zubir NA, Yacou C, Zhang X et al (2014) Optimisation of graphene oxide–iron oxide nanocomposite in heterogeneous Fenton-like oxidation of Acid Orange 7. J Environ Chem Eng 2(3):1881–1888
59. Chang YH, Yao YF, Luo H et al (2014) Magnetic Fe3O4-GO nanocomposites as highly efficient Fenton-like catalyst for the degradation of dyes. Int J Nanomanuf 10(1–2):132–141
60. Liu W, Qian J, Wang K et al (2013) Magnetically separable Fe3O4 nanoparticles-decorated reduced graphene oxide nanocomposite for catalytic wet hydrogen peroxide oxidation. J Inorg Organomet P 23(4):907–916
61. Zhou Z, Su M, Shih K (2017) Highly efficient and recyclable graphene oxide-magnetite composites for isatin mineralization. J Alloy Compd 725:302–309

62. Qiu B, Li Q, Shen B et al (2016) Stöber-like method to synthesize ultradispersed Fe3O4 nanoparticles on graphene with excellent Photo-Fenton reaction and high-performance lithium storage. Appl Catal B-Environ 183:216–223
63. Jiang X, Li L, Cui Y et al (2017) New branch on old tree: green-synthesized RGO/Fe3O4 composite as a photo-Fenton catalyst for rapid decomposition of methylene blue. Ceram Int 43 (16):14361–14368
64. Yu L, Chen J, Liang Z et al (2016) Degradation of phenol using Fe3O4-GO nanocomposite as a heterogeneous photo-Fenton catalyst. Sep Purif Technol 171:80–87
65. Boruah PK, Sharma B, Karbhal I et al (2017) Ammonia-modified graphene sheets decorated with magnetic Fe3O4 nanoparticles for the photocatalytic and photo-Fenton degradation of phenolic compounds under sunlight irradiation. J Hazard Mater 325:90–100
66. Wang P, Wang L, Sun Q et al (2016) Preparation and performance of Fe3O4@hydrophilic graphene composites with excellent Photo-Fenton activity for photocatalysis. Mater Lett 183:61–64
67. Yang B, Tian Z, Zhang L et al (2015) Enhanced heterogeneous Fenton degradation of Methylene Blue by nanoscale zero valent iron (nZVI) assembled on magnetic Fe3O4/reduced graphene oxide. J Water Process Eng 5:101–111
68. Zubir NA, Yacou C, Motuzas J et al (2014) Structural and functional investigation of graphene oxide-Fe3O4 nanocomposites for the heterogeneous Fenton-like reaction. Sci Rep 4:4594
69. He H, Huang J, Lu J (2016) Photo-and Photo-Fenton-like catalytic degradations of Malachite Green in a water using magnetically separable ZnFe2O4-reduced graphene oxide hybrid nanostructures. J Sci Res Rep 10(2):1–11
70. Yao Y, Cai Y, Lu F et al (2014) Magnetic recoverable MnFe2O4 and MnFe2O4-graphene hybrid as heterogeneous catalysts of peroxymonosulfate activation for efficient degradation of aqueous organic pollutants. J Hazard Mater 270:61–70
71. Yao Y, Yang Z, Zhang D et al (2012) Magnetic CoFe2O4-graphene hybrids: facile synthesis, characterization, and catalytic properties. Ind Eng Chem Res 51(17):6044–6051
72. Yang D, Feng J, Jiang L et al (2015) Photocatalyst interface engineering: spatially confined growth of ZnFe2O4 within graphene networks as excellent visible-light-driven photocatalysts. Adv Funct Mater 25(45):7080–7087
73. Fu Y, Wang X (2011) Magnetically separable ZnFe2O4-graphene catalyst and its high photocatalytic performance under visible light irradiation. Ind Eng Chem Res 50 (12):7210–7218
74. Lu D, Zhang Y, Lin S et al (2013) Synthesis of magnetic ZnFe2O4/graphene composite and its application in photocatalytic degradation of dyes. J Alloy Compd 579:336–342
75. Wang Y, Fang J, Crittenden JC et al (2017) Novel RGO/α-FeOOH supported catalyst for Fenton oxidation of phenol at a wide pH range using solar-light-driven irradiation. J Hazard Mater 329:321–329
76. Liu Y, Liu X, Zhao Y et al (2017) Aligned α-FeOOH nanorods anchored on a graphene oxide-carbon nanotubes aerogel can serve as an effective Fenton-like oxidation catalyst. Appl Catal B-Environ 213:74–86